Early electrical field stimulation prevents the loss of spinal cord anterior horn motoneurons and muscle atrophy following spinal cord injury

Cheng Zhang[1, #], Wei Rong[2, #], Guang-Hao Zhang[1], Ai-Hua Wang[1], Chang-Zhe Wu[1], Xiao-Lin Huo[1, 3, *]
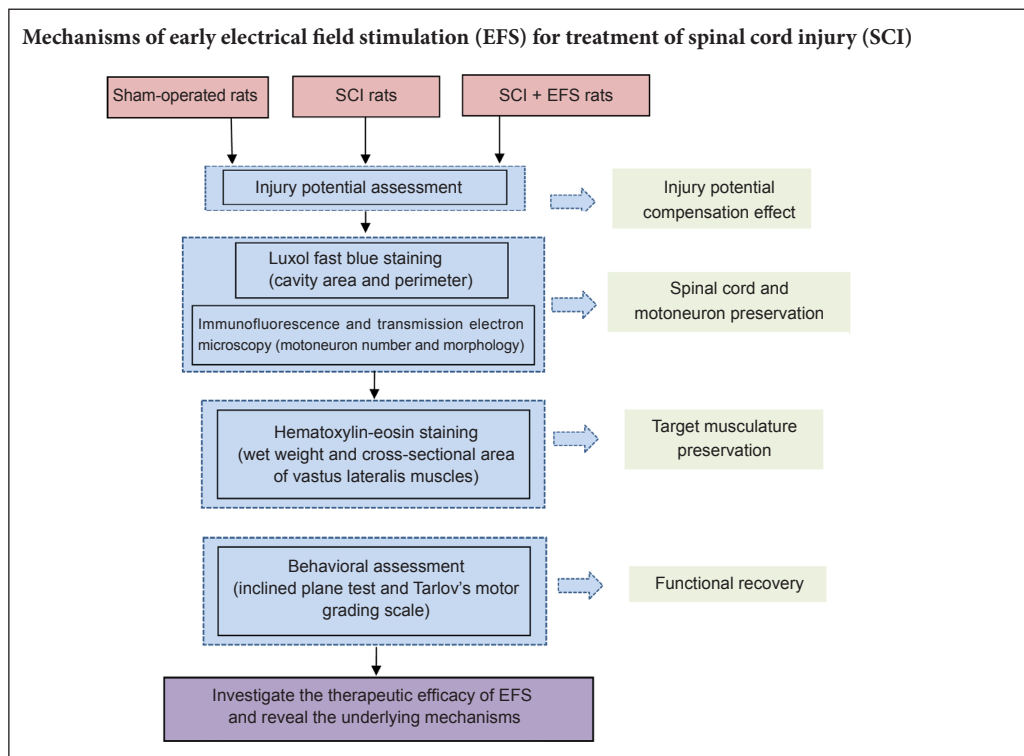
1 Beijing Key Laboratory of Bioelectromagnetism, Institute of Electrical Engineering, Chinese Academy of Sciences, Beijing, China
2 Department of Orthopedics, Beijing Tsinghua Changgung Hospital, Medical Center, Tsinghua University, Beijing, China
3 University of Chinese Academy of Sciences, Beijing, China

Graphical Abstract

Mechanisms of early electrical field stimulation (EFS) for treatment of spinal cord injury (SCI)

Correspondence to:
Xiao-Lin Huo, Ph.D.,
huoxl@mail.iee.ac.cn.

#These authors contributed equally to this work.

orcid:
0000-0001-7416-3601
(Xiao-Lin Huo)

Abstract

Our previous study revealed that early application of electrical field stimulation (EFS) with the anode at the lesion and the cathode distal to the lesion reduced injury potential, inhibited secondary injury and was neuroprotective in the dorsal corticospinal tract after spinal cord injury (SCI). The objective of this study was to further evaluate the effect of EFS on protection of anterior horn motoneurons and their target musculature after SCI and its mechanism. Rats were randomized into three equal groups. The EFS group received EFS for 30 minutes immediately after injury at T_{10}. SCI group rats were only subjected to SCI and sham group rats were only subjected to laminectomy. Luxol fast blue staining demonstrated that spinal cord tissue in the injury center was better protected; cross-sectional area and perimeter of injured tissue were significantly smaller in the EFS group than in the SCI group. Immunofluorescence and transmission electron microscopy showed that the number of spinal cord anterior horn motoneurons was greater and the number of abnormal neurons reduced in the EFS group compared with the SCI group. Wet weight and cross-sectional area of vastus lateralis muscles were smaller in the SCI group to in the sham group. However, EFS improved muscle atrophy and behavioral examination showed that EFS significantly increased the angle in the inclined plane test and Tarlov's motor grading score. The above results confirm that early EFS can effectively impede spinal cord anterior horn motoneuron loss, promote motor function recovery and reduce muscle atrophy in rats after SCI.

Introduction

Spinal cord injury (SCI) is damage to the spinal cord that, depending on the injury level and severity, can produce severe impairments of motor function at and below the level of the damage (McDonald and Sadowsky, 2002; Lynskey et al., 2008; David and Steward, 2010). Although spontaneous regeneration is rare in the adult spinal cord, the central nervous system is able to show significant functional recovery from incomplete SCI with appropriate treatment (Raineteau and Schwab, 2001; Han et al., 2015; Li et al., 2015).

It is believed that secondary injury processes including programmed cellular apoptosis are activated in the spinal cord after SCI (David and Kroner, 2011; Zhang et al., 2012). Cellular apoptosis aggravates irreversible tissue damage and function loss that worsens the primary spinal cord lesion (Borgens, 2012; Oudega, 2012; Rong et al., 2012). Neuronal apoptosis at the lesion site has been revealed (Liu et al., 1997). An extensive study confirmed the spatial and temporal profiles of the loss of neurons (Kieran and Greensmith, 2004). A main trigger for apoptosis seems to be injury-induced Ca^{2+} influx that exceeds the homeostatic capacity of cells and ultimately triggers cell apoptosis in the tissue surrounding the injury (Oyinbo, 2011; Rong et al., 2012). Many agents that impede Ca^{2+} influx-induced injury have shown protective function after nerve injuries (Liverman et al., 2005; Yan et al., 2010).

Furthermore, Ca^{2+} influx is also the main cause of injury potential, which refers to a direct current voltage between the normal and damaged tissue (Goodman et al., 1985; Zuberi et al., 2008). Our recent investigations elaborated a positive correlation between the damage potential and injury severity. The injury potential increased quickly within 30 minutes after the damage and then decreased gradually to 0 mV several hours after injury (Zhang et al., 2013). Electrical field stimulation (EFS) treatment with the anode at the lesion and the cathode distal to the lesion offset the Ca^{2+} influx and accordingly delayed and reduced the formation of injury potential. The results revealed that EFS could efficiently exert neuroprotective effects against apoptosis and promote axon regeneration in the dorsal corticospinal tract of the spinal cord after SCI (Zhang et al., 2015a).

Secondary damage continues for weeks following SCI and some neurons, including anterior horn motoneurons, may be eventually damaged (Liu and Xu, 2010; Pastor et al., 2014; Liu et al., 2016) and the ventral roots may also be involved (Moschilla et al., 2001; Karalija et al., 2012). Some studies have reported that the muscles supplied by spinal cord motoneurons and the motor nerves through the ventral roots at and distal to the injury level undergo denervation and atrophy (Gordon and Mao, 1994; Byers et al., 2012). The recovery process after injury depends not only on the motoneurons in the spinal cord but also their target musculature. Therefore, the objective of this study was to further evaluate the neuroprotective efficacy of early EFS on functional recovery. We also evaluated the effect of EFS on protecting spinal anterior horn motoneurons and lower limb musculature after severe SCI.

Materials and Methods

Animals

Fifty-four female Sprague-Dawley rats aged 8 weeks and weighing 200–220 g were bought from Beijing HFK Bio-Technology (Beijing, China; animal produce license No. SCXK (Jing) 2014-0004). The study protocol was approved by the Animal Welfare Committee of Beijing Key Laboratory of Bioelectromagnetism. The experimental procedures followed *the United States National Institutes of Health Guide for the Care and Use of Laboratory Animal* (NIH Publication No. 85-23, revised 1985).

The 54 rats were equally randomized into three groups. EFS group rats received EFS immediately after SCI; T_8, T_{10}, and T_{12} spinal cord segments were exposed. One electric field stimulator contains one anode and two cathodes, and each rat received stimulation from two electrical field stimulators. Two anodes were sutured at both sides of the T_{10} paravertebral muscle, and four cathodes were sutured at both sides of T_8 and T_{12} paravertebral muscle (**Figure 1**). A severe impact injury at T_{10} (10 g, 50 mm) was induced by a trained technician using the weight-drop method (Zhang et al., 2015b). The electric field was applied (injury potential compensation) immediately after the measurement of injury potentials. The caudal and rostral injury potential was adjusted to 0 ± 0.5 mV. EFS lasted for 30 minutes. All electrodes were removed following the stimulation. The rats of the SCI group were subjected to the same severe SCI procedures but without electric field stimulator suture and electric field stimulation. The sham group rats were subjected to the same procedure of laminectomy without weight-drop injury and electric field stimulation.

Electrical field stimulation and injury potential measurement system

The electrical field stimulation system and the injury potential measurement system have been introduced comprehensively in our previous study (Zhang et al., 2015b); here we described them briefly.

Two 9-volt-batteries supplied energy for the electric field stimulator (Institute of Electrical Engineering, Chinese Academy of Sciences, Beijing, China). The central terminal of the potentiometer in the voltage regulation unit provided an electric potential between ± 0.43 V. The amplification unit included a noninverting amplifier, which could be adjusted from 1 to 21, and a voltage follower. The electrode system was composed of one spiral reference electrode and two spiral stimulating electrodes. A resistor was set up to limit the current flow in the tissues, which was between the output of the voltage follower and the stimulating electrode. Platinum-iridium (90:10) wires were used for each spiral electrode (**Figure 2**).

The injury potentials were measured by two glass electrodes. The upper glass tube of the glass electrode contained a calomel electrode and was filled with 3 M KCl solution. The lower glass tube was plugged by porous ceramic and filled with normal saline. The tip of one glass electrode was

gently placed at T_{10} and the tip of another glass electrode was lightly put on the surface of T_8 or T_{12}. The rostral injury potential (the voltage between T_8 and T_{10}) and the caudal injury potential (the voltage between T_{10} and T_{12}) were measured and recorded.

Luxol fast blue staining

At 8 weeks after the operation, the rats were executed by pentobarbital overdose (70 mg/kg; Abbott, North Chicago, IL, USA) and then transcardially perfused sequentially with 37°C phosphate buffered saline and cold 4% paraformaldehyde. The spinal cord segments (n = 5) compassing the injury center were removed and embedded in optimal cutting temperature compound (Sakura Finetek, Torrance, CA, USA). Serial spinal cord sagittal sections (20 μm thick, 500 μm intervals) were stained with luxol fast blue (ZSGB-Bio, Beijing, China). Transverse sections of spinal cord showing the largest proportion of cavity were taken to represent the injury center. The cavity area and perimeter of injured spinal cord were measured with Image Pro Plus 5.0 software (Cybernetics, Rockville, MD, USA).

Immunofluorescence assessment

Eight weeks after the injury, spinal cord frozen sections (5 μm, n = 5/group) 2 mm caudal from the epicenter were prepared for immunofluorescence staining. Motoneurons in the anterior horn were marked by a rabbit anti-choline acetyltransferase (ChAT) antibody (1:500; Millipore, Bedford, MA, USA) and a Red-X-conjugated goat anti-rabbit antibody (1:100; ZSGB-Bio, Beijing, China). Following immunostaining, all sections were coverslipped with 4′,6-diamidino-2-phenylindole (DAPI) (Southern Biotech, Birmingham, AL, USA) to stain the nuclei.

ChAT/DAPI co-labeled cells were counted in an area of the bottom right and bottom left quarter of the spinal cord gray matter. The quarter areas were defined by vertical and horizontal crossed lines, which were drawn through the central canal (Ling et al., 2013). Photos from the anterior horn were taken by a fluorescence microscope (Nikon E600, Tokyo, Japan). ChAT/DAPI co-labeled cells were counted in three randomized fields (450 μm × 450 μm) of 10 sections per group (30 optical fields per group). The motoneuron quantity in each group was expressed as the mean cell number per mm^2.

Transmission electron microscopy

Spinal cords (n = 3/group) 2 mm caudal from the center were fixed in 2.5% glutaraldehyde and 2% osmic acid (Klamar, Shanghai, China) 8 weeks after the injury. The spinal cords were embedded in epoxy resin and ultrathin sections mounted on copper grids were observed using transmission electron microscopy (Hitachi-7650, Tokyo, Japan).

Five grids in different parts of the gray matter in the anterior horn were prepared in each group. The morphological alterations of the nucleus and chromatin condensation were assessed in approximately 20 motoneurons from rats of each group.

Wet weight and cross-sectional area of vastus lateralis muscles

The target musculature (n = 5/group) of the motoneurons were further examined to evaluate regressive muscle changes post-injury. The bilateral vastus lateralis muscles were removed 4 and 8 weeks post-injury and their wet weights were measured.

The cross-sectional area of hematoxylin and eosin (ZSGB-Bio, Beijing, China) stained sections (10 μm) of vastus lateralis muscles were examined and approximately 150 muscle fibers per rat were evaluated.

Behavioral assessment

Assessment of functional recovery was performed independently by two investigators before injury and once per week until 8 weeks after SCI (n = 13/group).

The inclined plane test was used to evaluate the ability of the rats to maintain postural stability (Rivlin and Tator, 1977; Pal et al., 2010). The rats stood on an inclined plane, which was tilted slowly, and the maximum angle that the rats could hold their position for 5 seconds was considered as the final incline.

The modified Tarlov's motor grading scale was used to evaluate motor function (Behrmann et al., 1992; Liu et al., 2011): grade 5, rats can walk normally; grade 4, rats can walk with uncoordinated hind limbs; grade 3, rats can stand but cannot walk; grade 2, rats cannot stand but can slightly perform voluntary hind limb activity; grade 1, rats have no voluntary hind limb activity. Three measurements were taken for each rat, and the average angle and scores were calculated.

Statistical analysis

All data were expressed as the mean ± SD, and analyzed using SPSS 15.0 software (SPSS, Chicago, IL, USA). One-way analysis of variance followed by Tukey's *post hoc* test was used to compare the indexes among groups. Repeated-measures analysis of variance followed by Bonferroni's *post hoc* test, unless otherwise stated, was used to compare the indexes of groups over time. A *P* value of < 0.05 was considered statistically significant.

Results

Injury potential compensation by EFS

The rostral and caudal injury potentials of the SCI group rats increased rapidly with the onset of injury, and then decreased gradually until approximately 30 minutes post-injury. EFS group rats were given simulation (injury potential compensation) immediately following SCI. The injury potential of the EFS group was 0.5 mV because of injury potential compensation. The compensation voltages were 2.7 ± 0.1 V, and the amount of current was 400 ± 10 μA during EFS (**Figure 3A**).

At the end of stimulation, the stitched electrodes were removed; injury potential restarted and then gradually decreased to 60 minutes post-injury. The rostral and caudal injury potentials of the SCI group were 4.21 ± 1.77 mV and 5.86 ± 1.86 mV, respectively, 60 minutes post-injury (**Figure 3B**)
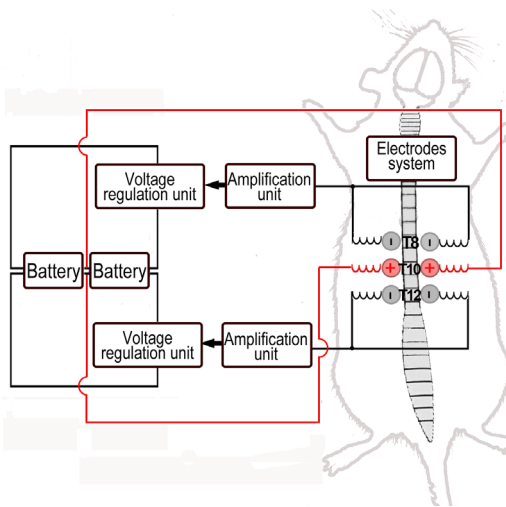
Figure 1 Stimulation setup.
(A) Schematic diagram of the applied electric field stimulator. (B) Electrode suture method. The cathodes were sutured at the paravertebral muscle of T_8 and T_{12}, whereas the anodes were sutured at T_{10}.
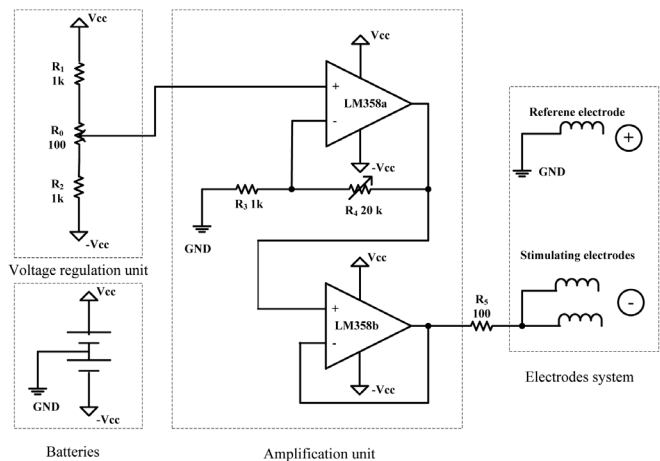

Figure 2 Schematic of the applied electrical field stimulator.
The electric field stimulator was powered by two 9 V batteries. A voltage regulation unit comprising R0, R1, and R2 provided a voltage range between ± 0.43 V. The amplification unit included a noninverting amplifier and a voltage follower. Two stimulating electrodes and one reference electrode comprised the electrode system. GND: Ground; R: resistance; Vcc: volt current condenser.
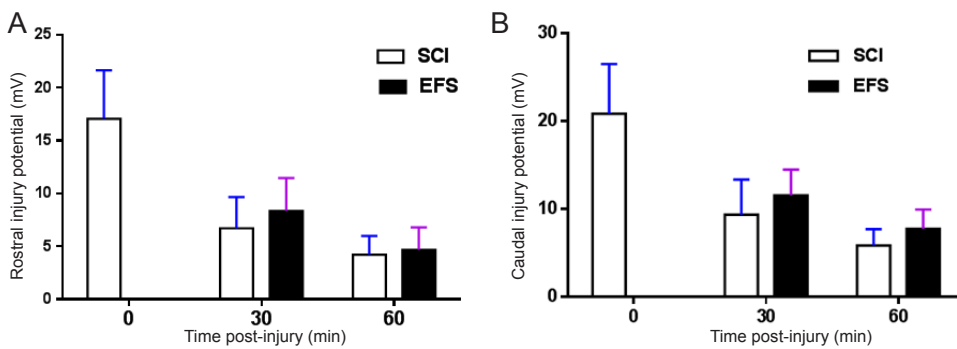
Figure 3 Injury potential compensation by EFS
(A, B) Rostral and caudal injury potentials of the SCI and EFS groups. The rostral and caudal injury potentials of the SCI group rats increased rapidly with the onset of injury and then decreased gradually approximately 30 minutes post-injury. At the end of the stimulation, the stitched electrodes were removed; injury potential restarted, then gradually decreased 60 minutes post-injury. EFS: Electrical field stimulation; SCI: spinal cord injury; min: minute.
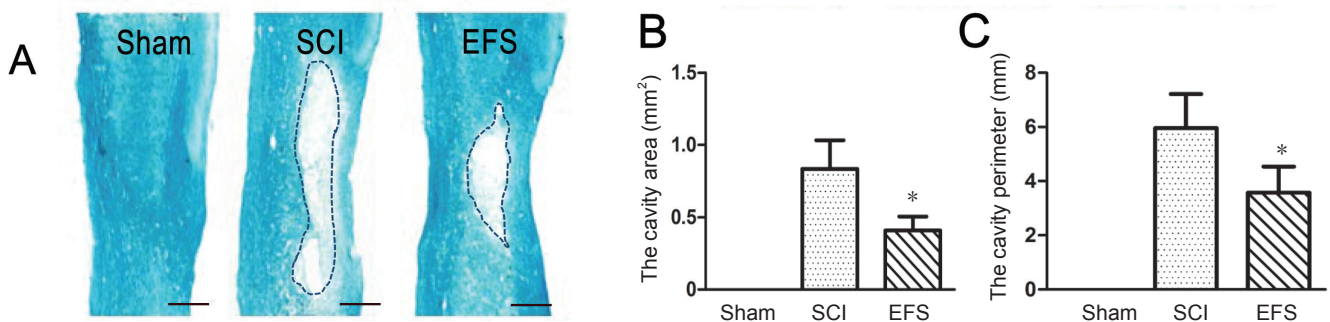

Figure 4 Spinal cord tissue preservation at the injury center 8 weeks post-injury.
(A) Luxol fast blue staining of 20 μm sagittal sections from three groups of rats. The dotted lines in the images indicate the border of the lesion area. Scale bars: 100 mm. (B) Quantitative data on the cavity area of injured spinal cord. (C) Quantitative data on the cavity perimeter of injured spinal cord; *$P < 0.05$, *vs*. SCI group (mean ± SD, $n = 5$, one-way analysis of variance followed by Tukey's *post hoc* test). EFS: Electrical field stimulation; SCI: spinal cord injury.

Luxol fast blue staining

Characteristic cavitation was produced by damage in EFS and SCI groups at the injury center. The degree of tissue disruption was high in the SCI group. Significant tissue preservation and decreased cavity expansion were seen in the EFS group (**Figure 4A**). The cavity area ($F_{0.05(2,12)} = 3.88$, $F = 5.03$, $P < 0.05$) and perimeter ($F_{0.05(2,12)} = 3.88$, $F = 6.18$, $P < 0.05$)

were larger in the SCI group than in the EFS group (**Figure 4B, C**).

Immunofluorescence assessment of spinal anterior horn motoneurons

To evaluate the protective effect of EFS on anterior horn motoneurons, spinal cord sections 2 mm caudal from the
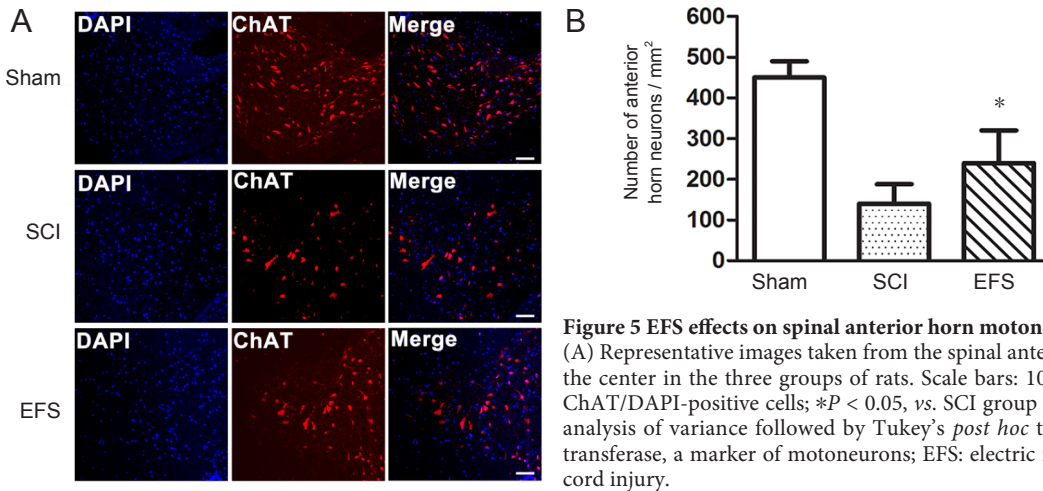
Figure 5 EFS effects on spinal anterior horn motoneurons 8 weeks post-injury.
(A) Representative images taken from the spinal anterior horn 2 mm caudal from the center in the three groups of rats. Scale bars: 100 μm. (B) Quantification of ChAT/DAPI-positive cells; *$P < 0.05$, *vs.* SCI group (mean ± SD, $n = 5$, one-way analysis of variance followed by Tukey's *post hoc* test). ChAT: Choline acetyltransferase, a marker of motoneurons; EFS: electric field stimulation; SCI: spinal cord injury.
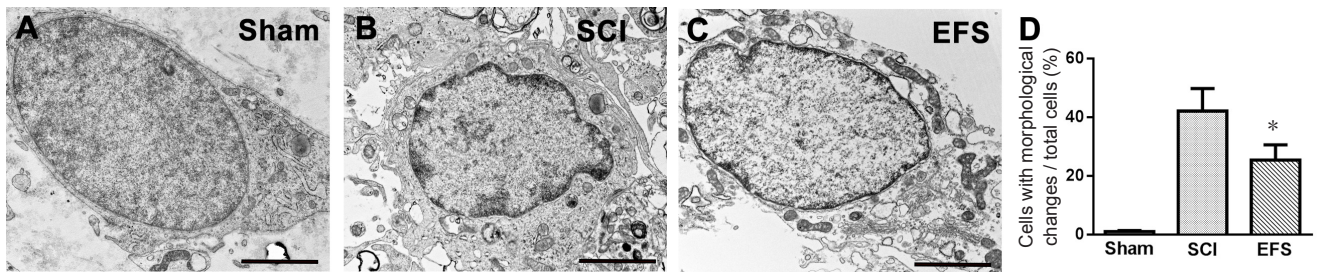

Figure 6 EFS effects on ultrastructure of spinal cord anterior horn neurons 2 mm caudal from the injury center 8 weeks post-injury.
(A) In the sham group, the shape of neuronal nuclei was almost normal. (B) In the SCI group, some anterior horn neurons had morphological alterations (cell shrinkage and chromatin condensation). (C) In the EFS group, the extent of chromatin condensation and the shape of mitochondria were much better than in the SCI group. Scale bars: 2 μm. (D) The proportion of the cells with morphological alterations in the EFS group was significantly lower than that in the SCI group; *$P < 0.05$, *vs.* SCI group (mean ± SD, $n = 3$, one-way analysis of variance followed by Tukey's *post hoc* test). EFS: Electrical field stimulation; SCI: spinal cord injury.
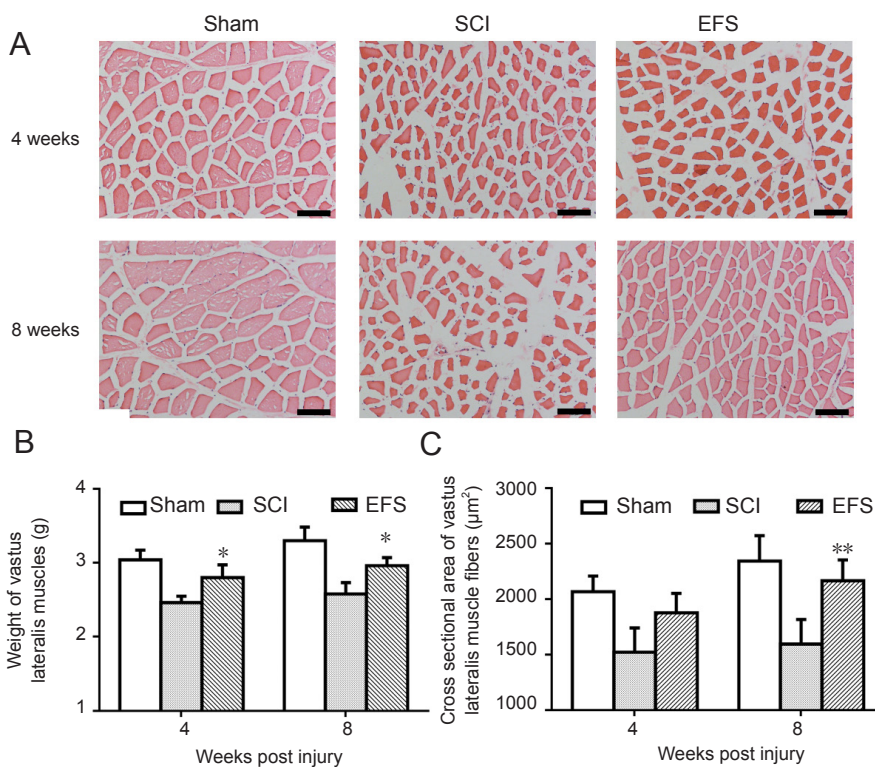

Figure 7 EFS effects on wet weight and cross-sectional area of vastus lateralis muscle fibers 4 and 8 weeks after SCI.
(A) Light micrographs of transversely sectioned vastus lateralis muscles 4 and 8 weeks after the SCI. Scale bars: 100 μm. (B) Wet weight of vastus lateralis muscles was significantly lower in the SCI group than in the EFS group. (C) The mean cross sectional area of vastus lateralis muscle fibers was significantly smaller in the SCI group than in the EFS group; *$P < 0.05$, **$P < 0.01$, *vs.* SCI group (mean ± SD, $n = 5$, one-way analysis of variance followed by Tukey's *post hoc* test). EFS: Electrical field stimulation; SCI: spinal cord injury.
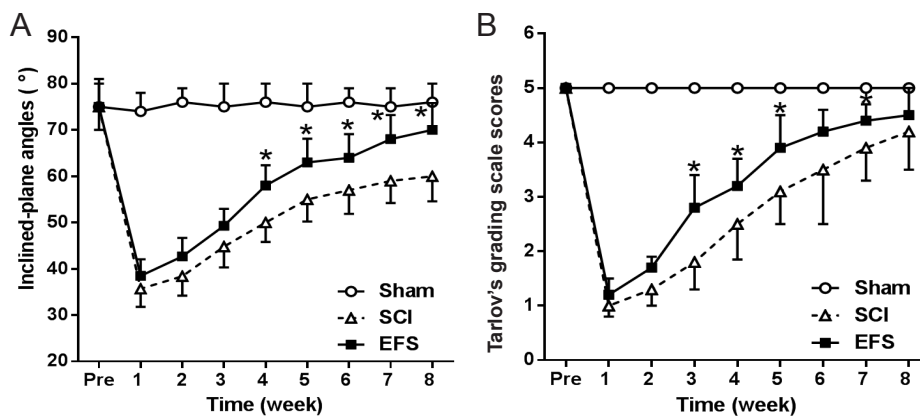
Figure 8 EFS effect on behavioral outcome of rats from three groups.
(A) The inclined-plane test after SCI. (B) Modified Tarlov's grading scale after SCI. Functional recovery was assessed before injury and once per week until 8 weeks after SCI. Significant functional improvement was observed in the EFS group; ∗$P < 0.05$, *vs.* SCI group (mean ± SD, $n = 13$, repeated-measures analysis of variance followed by Bonferroni's *post hoc* test). EFS: Electric field stimulation; SCI: spinal cord injury; Pre: pre-injury.

center were immunostained for ChAT, a marker of motoneurons. The number of ChAT/DAPI-positive cells was quantified in the spinal anterior horn (**Figure 5A**). The statistical results showed that the EFS group rats preserved spinal anterior horn motoneurons better than the rats in the SCI group 8 weeks post-injury ($F_{0.05(2,12)} = 3.88$, $F = 4.05$, $P < 0.05$) (**Figure 5B**).

Ultrastructure in the spinal anterior horn after SCI
Transmission electron microscopy revealed that the shape of neuronal nuclei was normal and the mitochondria contained sparse cristae in the sham group (**Figure 6A**). At 8 weeks after injury, in the SCI group spinal anterior horn motoneurons had morphological changes, such as cell shrinkage and chromatin condensation (**Figure 6B**). In the EFS group, the distributions of organelles were more normal and the shapes of motoneurons were better preserved (**Figure 6C**). The proportion of cells with morphological alterations in the EFS group was significantly lower than that in the SCI group ($F_{0.05(2,6)} = 5.14$, $F = 7.82$, $P < 0.05$) (**Figure 6D**).

Wet weight and cross-sectional area changes of vastus lateralis muscle fibers
The degree of vastus lateralis muscle loss was estimated among the three groups of rats (**Figure 7B**). The SCI group showed significantly lower wet weights compared with the EFS group at 4 ($F_{0.05(2,12)} = 3.88$, $F = 6.37$, $P < 0.05$) and 8 ($F_{0.05(2,12)} = 3.88$, $F = 5.47$, $P < 0.05$) weeks after the injury.

Hematoxylin-eosin stained micrographs of transversely sectioned vastus lateralis muscle further showed that SCI caused vastus lateralis muscle fiber atrophy in both injury groups after SCI (**Figure 7A**). Cross-sectional areas in the injured groups initially became smaller. The mean area of the SCI group was significantly smaller than the EFS group at 4 ($F_{0.05(2,12)} = 3.88$, $F = 6.37$, $P < 0.05$) and 8 ($F_{0.01(2,12)} = 6.93$, $F = 11.25$, $P < 0.01$) weeks (**Figure 7C**).

Locomotor function testing after SCI
The mean angles of all groups of rats in the inclined-plane test were approximately 75.00° preoperatively. The mean inclined-plane angles decreased and were then followed by a slow decline in both SCI and EFS groups after SCI. Four

weeks after injury, the angles recorded in the SCI and EFS groups were 50.21 ± 4.27° and 58.24 ± 4.35°, respectively. The angles were significantly larger in the EFS group than in the SCI group and this advantage persisted until the end of the study ($F_{0.05(2,21)} = 3.47$, $F = 5.26$, $P < 0.05$) (**Figure 8A**). The angles of the sham rats were approximately 75.00°.

All the rats were graded according to the modified Tarlov's grading scale standard (**Figure 8B**). The motor scores were 5.0 ± 0.0 in all groups before the injury. After injury, the injury ranking dropped and then gradually elevated. At 3, 4, 5 and 7 weeks, grading scores were significantly better in the EFS group than in the SCI group ($F_{0.05(2,21)} = 3.47$, $F = 4.48$, $P < 0.05$). At 8 weeks, the grades of the SCI and EFS groups reached the maximal ranking, but the difference between them was not statistically significant.

Discussion
Electrical fields (10 mV/mm) could adjust Ca^{2+} migration into injured lamprey spinal axons, and the appropriate polarity of the electric field nearly canceled out the migration of Ca^{2+} at the injury end (Strautman et al., 1990). Accordingly, we conducted applied EFS (270 mV/mm) with the anode at the lesion site and the cathode distal to the lesion in injured spinal cord. The larger electrical field used in the present study may help offset the Ca^{2+} flux at injured regions. In our previous paper, we demonstrated neuroprotective effects of EFS and satisfactory results were obtained in the dorsal corticospinal tract of spinal cord post-injury (Zhang et al., 2015a).

SCI has been characterized by morphological hallmarks such as the loss of spinal cord tissue, including motoneurons (Sharp et al., 2010; Bains et al., 2012). In this study, luxol fast blue staining was performed 8 weeks after injury and the degree of white and gray tissue preservation was high in the EFS group. The presence of ChAT reliably reveals motoneurons (Xu et al., 2011; Sareen et al., 2012), so motoneurons were stained for ChAT and then quantified. The results confirmed that EFS significantly preserved the number of spinal cord anterior horn motoneurons 8 weeks post injury. Furthermore, results from transmission electron microscopy showed that EFS maintained the configuration of spinal cord anterior horn motoneurons 8 weeks after injury.

The proportion of cells with morphological alterations was significantly lower in the EFS group than in the SCI group. These results indicate that EFS played an important role in neuroprotection of anterior horn motoneurons after SCI.

Muscle atrophy shown by weight and fiber size is typical of weight-bearing muscles that are innervated by spinal cord motoneurons below the lesion level after SCI (Peckham et al., 1976; Giangregorio and McCartney, 2006; Panisset et al., 2016). As expected, in the present study the injured rats exhibited vastus lateralis muscle atrophy, as shown by wet weight and cross-sectional area measurement at 4 and 8 weeks after SCI. However, the regressive changes of vastus lateralis muscle in the EFS group were prevented by EFS treatment. The results indicated better wet weight and morphology of vastus lateralis muscle in the EFS group than in the SCI group. This effect may be due to sparing of motoneuron function with EFS treatment after SCI (Morimoto, 2012; Jain, 2016).

Large motor deficits persist for a long time after SCI, and poor functional recovery of SCI groups has been shown by behavioral assessment (Rengachary et al., 2011; Kolb, 2013). Lower behavior assessment scores indicate a poorer ability to maintain postural stability and motor function (Marigold et al., 2004; Liu et al., 2011). After EFS intervention, behavioral recovery was improved and the magnitude of locomotor recovery was strongly paralleled by the extent of spared motoneurons (Mondello et al., 2015). This improvement was actually an increase of coordinated activity among the various muscles of the hind limbs, which could be attributed locally to sparing of enough spinal circuitry to maintain motor vitality and to prevent target muscle atrophy (Martin et al., 2012; Roy et al., 2012; Slawinska et al., 2014).

One limitation of the present study was the lack of a sham EFS group. To ensure that the neuroprotective effect was not the result of the EFS setup but indeed was the result of the EFS, a sham EFS group with exactly the same EFS setup should be conducted in our future experiments.

In summary, EFS with the anode at the lesion and the cathode distal to the lesion efficiently protected anterior horn motoneurons against apoptosis and vastus lateralis muscles from atrophy. The differences in the spinal cord and vastus lateralis muscle analyses correlated with greater functional improvement of EFS group rats at the endpoint. This kind of physical therapy will be valuable for acute SCI treatment.

References

Bains M, Hall ED (2012) Antioxidant therapies in traumatic brain and spinal cord injury. BBA-Mol Basis Dis 1822:675-684.

Behrmann DL, Bresnahan JC, Beattie MS, Shah BR (1992) Spinal cord injury produced by consistent mechanical displacement of the cord in rats: behavioral and histologic analysis. J Neurotrauma 9:197-217.

Borgens RB (2012) Understanding second injury. Q Rev Biol 87:39.

Byers JS, Huguenard AL, Kuruppu D, Liu NK, Xu XM, Sengelaub DR (2012) Neuroprotective effects of testosterone on motoneuron and muscle morphology following spinal cord injury. J Comp Neurol 520:2683-2696.

David BT, Steward (2010) Deficits in bladder function following spinal cord injury vary depending on the level of the injury. Exp Neurol 226:128-135.

David S, Kroner A (2011) Repertoire of microglial and macrophage responses after spinal cord injury. Nat Rev Neurosci 12:388-399.

Giangregorio L, McCartney N (2006) Bone loss and muscle atrophy in spinal cord injury: epidemiology, fracture prediction, and rehabilitation strategies. J Spinal Cord Med 29:489-500.

Goodman RM, Wachs K, Keller S, Black P (1985) Spontaneous spinal cord "injury potential" in the rat. Neurosurgery 17:4.

Gordon T, Mao J (1994) Muscle atrophy and procedures for training after spinal cord injury. Phys Ther 74:50-60.

Han S, Wang B, Jin W, Xiao Z, Li X, Ding W, Kapur M, Chen B, Yuan B, Zhu T, Wang H, Wang J, Dong Q, Liang W, Dai J (2015) The linear-ordered collagen scaffold-BDNF complex significantly promotes functional recovery after completely transected spinal cord injury in canine. Biomaterials 41:89-96.

Jain KK (2016) Regenerative therapy for central nervous system trauma. Springer International Publishing.

Karalija A, Novikova LN, Kingham PJ, Wiberg M, Novikov LN (2012) Neuroprotective effects of N-acetyl-cysteine and acetyl-L-carnitine after spinal cord injury in adult rats. PLoS One 7:e41086.

Kieran D, Greensmith L (2004) Inhibition of calpains, by treatment with leupeptin, improves motoneuron survival and muscle function in models of motoneuron degeneration. Neuroscience 125:427-439.

Kolb B (2013) Brain plasticity and behavior. Lethbridge: Psychology Press, Canada.

Li L, Guo JD, Wang HD, Shi YM, Yuan YL, Hou SX (2015) Prohibitin 1 gene delivery promotes functional recovery in rats with spinal cord injury. Neuroscience 286:27-36.

Ling X, Bao F, Qian H, Liu D (2013) The temporal and spatial profiles of cell loss following experimental spinal cord injury: effect of antioxidant therapy on cell death and functional recovery. BMC Neurosci 14:146-183.

Liu C, Shi Z, Fan L, Zhang C, Wang K, Wang B (2011) Resveratrol improves neuron protection and functional recovery in rat model of spinal cord injury. Brain Res 1374:100-109.

Liu J, Tang T, Yang H (2011) Protective effect of deferoxamine on experimental spinal cord injury in rat. Injury 42:742-745.

Liu JM, Wang FC, Zhou YJ, Mu L, Hou SK, Hao LN, Zhang ZT (2016) Effect of electroacupuncture stimulation on apoptosis of nerve cells in a rat model of spinal cord contusion. Zhongguo Zuzhi Gongcheng Yanjiu 20:616-621.

Liu NK, Xu XM (2010) Phospholipase A2 and its molecular mechanism after spinal cord injury. Mol Neurobiol 41:197-205.

Liu XZ, Xu XM, Hu R, Du C, Zhang SX, McDonald JW, Dong HX, Wu YJ, Fan GS, Jacquin MF, Hsu CY, Choi DW (1997) Neuronal and glial apoptosis after traumatic spinal cord injury. J Neurosci 17:5395-5406.

Liverman TC, Altevogt MB, Joy EJ, Johnson TR (2005) Spinal cord injury: progress, promise, and priorities. National Academy of Sciences N.W. Washington, DC, USA.

Lynskey JV, Belanger A, Jung R (2008) Activity-dependent plasticity in spinal cord injury. J Rehabil Res Dev 45:229-240.

Marigold DS, Eng JJ, Tokuno CD, Donnelly CA (2004) Contribution of muscle strength and integration of afferent input to postural instability in persons with stroke. Neurorehabil Neural Repair 18:222-229.

Martin R, Sadowsky C, Obst K, Meyer B, McDonald J (2012) Functional electrical stimulation in spinal cord injury: from theory to practice. Top Spinal Cord Inj Rehabil 18:28-33.

McDonald JW, Sadowsky C (2002) Spinal-cord injury. Lancet 359:417-425.

Mondello SE, Sunshine MD, Fischedick AE, Moritz CT, Horner PJ (2015) A cervical hemi-contusion spinal cord injury model for the investigation of novel therapeutics targeting proximal and distal forelimb functional recovery. J Neurotraum 32:1994-2007.

Morimoto T (2012) Role of electrical activity of neurons for neuroprotection. Int Rev Neurobiol 105:19-38.

Moschilla G, Song S, Chakera T (2001) Post-traumatic lumbar nerve root avulsion. Australas Radiol 45:281-284.

Oudega M (2012) Molecular and cellular mechanisms underlying the role of blood vessels in spinal cord injury and repair. Cell Tissue Res 349:269-288.

Oyinbo CA (2011) Secondary injury mechanisms in traumatic spinal cord injury: a nugget of this multiply cascade. Acta Neurobiol Exp (Wars) 71:19.

Pal R, Gopinath C, Rao NM, Banerjee P, Krishnamoorthy V, Venkataramana NK, Totey S (2010) Functional recovery after transplantation of bone marrow-derived human mesenchymal stromal cells in a rat model of spinal cord injury. Cytotherapy 12:792-806.

Panisset MG, Galea MP, El-Ansary D (2016) Does early exercise attenuate muscle atrophy or bone loss after spinal cord injury? Spinal Cord 54:84-92.

Pastor D, Viso-León MC., Botella-López A, Jaramillo-Merchan J, Moraleda JM, Jones J, Martínez S (2013) Bone marrow transplantation in hindlimb muscles of motoneuron degenerative mice reduces neuronal death and improves motor function. Stem Cells Dev 22:1633-1644.

Peckham PH, Mortimer JT, Marsolais EB (1976) Alteration in the force and fatigability of skeletal muscle in quadriplegic humans following exercise induced by chronic electrical stimulation. Clin Orthop Relat Res.

Raineteau O, Schwab ME (2001) Plasticity of motor systems after incomplete spinal cord injury. Nat Rev Neurosci 2:263-273.

Rengachary J, He BJ, Shulman GL, Corbetta M (2011) A behavioral analysis of spatial neglect and its recovery after stroke. Front Hum Neurosci 5:29-49.

Rivlin AS, Tator CH (1977) Objective clinical assessment of motor function after experimental spinal cord injury in the rat. J Neurosurg 47:577-581.

Rong W, Pan Y, Cai X, Song F, Zhao Z, Xiao SH, Zhang C (2017) The mechanism of Naringin-enhanced remyelination after spinal cord injury. Neural Regen Res 12:470-477.

Rong W, Wang J, Liu X, Jiang L, Wei F, Hu X, Liu Z (2012) Naringin treatment improves functional recovery by increasing BDNF and VEGF expression, inhibiting neuronal apoptosis after spinal cord injury. Neurochem Res 37:1615-1623.

Roy RR, Harkema SJ, Edgerton VR (2012) Basic concepts of activity-based interventions for improved recovery of motor function after spinal cord injury. Arch Phys Med Rehab 93:1487-1497.

Sareen D, Ebert AD, Heins BM, McGivern JV, Ornelas L, Svendsen CN (2012) Inhibition of apoptosis blocks human motor neuron cell death in a stem cell model of spinal muscular atrophy. PLoS One 7:e39113.

Sharp J, Frame J, Siegenthaler M, Nistor G, Keirstead HS (2010) Human embryonic stem cell-derived oligodendrocyte progenitor cell transplants improve recovery after cervical spinal cord injury. Stem Cells 28:152-163.

Slawinska U, Miazga K, Jordan LM (2014) The role of serotonin in the control of locomotor movements and strategies for restoring locomotion after spinal cord injury. Acta Neurobiol Exp (Wars) 74:172-187.

Strautman AF, Cork RJ, Robinson KR (1990) The distribution of free calcium in transected spinal axons and its modulation by applied electrical fields. J Neurosci Meth 10:3564-3575.

Xu L, Shen P, Hazel T, Johe K, Koliatsos VE (2011) Dual transplantation of human neural stem cells into cervical and lumbar cord ameliorates motor neuron disease in SOD1 transgenic rats. Neurosci Lett 494:222-226.

Yan JG, Matloub HS, Yan Y, Agresti M, Zhang LL, Jaradeh SS (2010) The correlation between calcium absorption and electrophysiological recovery in crushed rat peripheral nerves. Microsurgery 30:138-145.

Zhang C, Zhang G, Rong W, Wang A, Wu C, Huo X (2015a) Early applied electric field stimulation attenuates secondary apoptotic responses and exerts neuroprotective effects in acute spinal cord injury of rats. Neuroscience 291:260-271.

Zhang GH, Wang AH, Zhang C, Wu CZ, Bai JZ, Huo XL (2013) Compensation for injury potential by electrical stimulation after acute spinal cord injury in rat. Conf Proc IEEE Eng Med Biol Soc:3634-3637.

Zhang N, Yin Y, Xu SJ, Wu YP, Chen WS (2012) Inflammation and apoptosis in spinal cord injury. Indian J Med Res 135:287-296.

Zuberi M, Liu-Snyder P, Ul Haque A, Porterfield DM, Borgens RB (2008) Large naturally-produced electric currents and voltage traverse damaged mammalian spinal cord. J Biol Eng 2:11-27.

(Copyedited by Turnley A, Stow A, Wang J, Li CH, Qiu Y, Song LP, Zhao M)